Springer

Dear Author

Here are the proofs of your article.

- You can submit your corrections **online,** via **e-mail** or by **fax**.
- For **online** submission please insert your corrections in the online correction form. Always indicate the line number to which the correction refers.
- You can also insert your corrections in the proof PDF and **email** the annotated PDF.
- For **fax** submission, please ensure that your corrections are clearly legible. Use a fine black pen and write the correction in the margin, not too close to the edge of the page.
- Remember to note the **journal title**, **article number**, and **your name** when sending your response via e-mail or fax.
- **Check** the metadata sheet to make sure that the header information, especially author names and the corresponding affiliations are correctly shown.
- **Check** the questions that may have arisen during copy editing and insert your answers/corrections.
- **Check** that the text is complete and that all figures, tables and their legends are included. Also check the accuracy of special characters, equations, and electronic supplementary material if applicable. If necessary refer to the *Edited manuscript*.
- The publication of inaccurate data such as dosages and units can have serious consequences. Please take particular care that all such details are correct.
- Please **do not** make changes that involve only matters of style. We have generally introduced forms that follow the journal's style.
- Substantial changes in content, e.g., new results, corrected values, title and authorship are not allowed without the approval of the responsible editor. In such a case, please contact the Editorial Office and return his/her consent together with the proof.
- If we do not receive your corrections **within 48 hours**, we will send you a reminder.
- Your article will be published **Online First** approximately one week after receipt of your corrected proofs. This is the **official first publication** citable with the DOI. **Further changes are, therefore, not possible.**
- The **printed version** will follow in a forthcoming issue.

Please note

After online publication, subscribers (personal/institutional) to this journal will have access to the complete article via the DOI using the URL:

`http://dx.doi.org/10.1007/s00397-010-0507-0`

If you would like to know when your article has been published online, take advantage of our free alert service. For registration and further information, go to: http://www.springerlink.com.

Due to the electronic nature of the procedure, the manuscript and the original figures will only be returned to you on special request. When you return your corrections, please inform us, if you would like to have these documents returned.

Metadata of the article that will be visualized in OnlineFirst

Please note: Image will appear in color online but will be printed in black and white.

1	Article Title	**How polymeric solvents control shear inhomogeneity in large deformations of entangled polymer mixtures**	
2	Article Sub- Title		
3	Article Copyright - Year	**Springer-Verlag 2010 (This will be the copyright line in the final PDF)**	
4	Journal Name	Rheologica Acta	
5	Corresponding Author	Family Name	**Wang**
6		Particle	
7		Given Name	**Shi-Qing**
8		Suffix	
9		Organization	University of Akron
10		Division	Department of Polymer Science
11		Address	Akron 44325-3909, OH, USA
12		e-mail	swang@uakron.edu
13	Author	Family Name	**Ravindranath**
14		Particle	
15		Given Name	**Sham**
16		Suffix	
17		Organization	University of Akron
18		Division	Department of Polymer Science
19		Address	Akron 44325-3909, OH, USA
20		e-mail	
21	Author	Family Name	**Olechnowicz**
22		Particle	
23		Given Name	**M.**
24		Suffix	
25		Organization	University of Akron
26		Division	Department of Polymer Science
27		Address	Akron 44325-3909, OH, USA
28		e-mail	
29	Author	Family Name	**Chavan**
30		Particle	
31		Given Name	**V. S.**
32		Suffix	
33		Organization	University of Akron
34		Division	

35		Address	Department of Polymer Science Akron 44325-3909, OH, USA
36		e-mail	
37	Author	Family Name	**Quirk**
38		Particle	
39		Given Name	**R. P.**
40		Suffix	
41		Organization	University of Akron
42		Division	Department of Polymer Science
43		Address	Akron 44325-3909, OH, USA
44		e-mail	

45	Schedule	Received	25 May 2010
46		Revised	16 October 2010
47		Accepted	6 November 2010

48 Abstract

This work aims to elucidate how molecular parameters dictate the occurrence of inhomogeneous cohesive failure during step strain and large amplitude oscillatory shear (LAOS) respectively in entangled polymer mixtures. Based on three well-entangled polybutadiene (PB) mixtures, we perform simultaneous rheometric and particle-tracking velocimetric (PTV) measurements to illustrate how the slip length controls the degree of shear banding. Specifically, the PB mixtures were prepared using the same parent polymer ($M_w \cdot 10^6$ g/mol) at 10 wt.% concentration in respective polybutadiene solvents (PBS) of three different molecular weights 1.5, 10, and 46 K. After step strain, the entangled PB mixture with PBS-1.5 K displayed interfacial failure whereas the PB mixture with PBS-10 K showed bulk failure, demonstrating the effectiveness of our strategy to suppress wall slip by controlling PBS' molecular weight. Remarkably, the PBS-46K actually allows the elastic yielding to occur homogeneously so that no appreciable macroscopic motions were observed upon shear cessation. PBS is found to play a similar role in LAOS of these three PB mixtures. Finally, we demonstrate that in case of the slip-prone mixture based on PBS-1.5 K the interfacial failure could be drastically reduced by use of shearing plates with considerable surface roughness.

49	Keywords separated by ' - '	Nonlinear rheology - Entangled polymer solutions - Shear inhomogeneity - Elastic yielding - Wall slip
50	Foot note information	

Rheol Acta
DOI 10.1007/s00397-010-0507-0

ORIGINAL CONTRIBUTION

How polymeric solvents control shear inhomogeneity in large deformations of entangled polymer mixtures

Sham Ravindranath · Shi-Qing Wang · M. Olechnowicz · V. S. Chavan · R. P. Quirk

Received: 25 May 2010 / Revised: 16 October 2010 / Accepted: 6 November 2010

Abstract This work aims to elucidate how molecular parameters dictate the occurrence of inhomogeneous cohesive failure during step strain and large amplitude oscillatory shear (LAOS) respectively in entangled polymer mixtures. Based on three well-entangled polybutadiene (PB) mixtures, we perform simultaneous rheometric and particle-tracking velocimetric (PTV) measurements to illustrate how the slip length controls the degree of shear banding. Specifically, the PB mixtures were prepared using the same parent polymer ($M_w \sim 10^6$ g/mol) at 10 wt.% concentration in respective polybutadiene solvents (PBS) of three different molecular weights 1.5, 10, and 46 K. After step strain, the entangled PB mixture with PBS-1.5 K displayed interfacial failure whereas the PB mixture with PBS-10 K showed bulk failure, demonstrating the effectiveness of our strategy to suppress wall slip by controlling PBS' molecular weight. Remarkably, the PBS-46K actually allows the elastic yielding to occur homogeneously so that no appreciable macroscopic motions were observed upon shear cessation. PBS is found to play a similar role in LAOS of these three PB mixtures. Finally, we demonstrate that in case of the slip-prone mixture based on PBS-1.5 K the interfacial failure could be drastically reduced by use of shearing plates with considerable surface roughness.

S. Ravindranath · S.-Q. Wang (✉) · M. Olechnowicz · V. S. Chavan · R. P. Quirk
Department of Polymer Science, University of Akron, Akron, OH 44325-3909, USA
e-mail: swang@uakron.edu

Keywords Nonlinear rheology · Entangled polymer solutions · Shear inhomogeneity · Elastic yielding · Wall slip

Introduction

Response of entangled polymer mixtures to nonlinear deformations has been extensively studied in conventional rheometric setups such as cone-plate fixture, planar and circular Couette cells (Macosko 1994; Graessley 2008). These fixtures are capable of generating uniform shear rate across the gap and thereby can provide information about the constitutive behavior of entangled polymer mixtures. Until recently, shear deformation and flow of such materials had been assumed to occur homogeneously across the sample thickness in these apparatuses. Emerging particle-tracking velocimetric (PTV) observations in these fixtures recently indicated that this assumption is often violated: Upon a rapid startup shear, an entangled polymeric liquid first undergo elastic deformation before such a transient solid yields to allow permanent (irrecoverable) deformation, i.e., flow. Apparently, after the shear stress overshoot (i.e., the yield point), the quasi-elastic "solid", unable to sustain indefinite amount of deformation, can collapse in an inhomogeneous manner (Tapadia and Wang 2006; Boukany and Wang 2007; Hu et al. 2007; Ravindranath and Wang 2008a, b; Ravindranath and Wang 2007a). Sufficiently entangled polymers also show shear banding in large amplitude oscillatory shear (LAOS; Tapadia et al. 2006; Ravindranath and Wang 2008a, b). Finally and most strikingly, inhomogeneous breakup was discovered for both entangled mixtures (Wang et al. 2006; Ravindranath and Wang 2007b) and

melts (Boukany et al. 2009b) after large step strain in both simple shear and uniaxial extension (Wang et al. 2007a, b). On the other hand, the "solid" character diminishes when the level of chain entanglement is reduced. Consequently, less-entangled liquids can avoid shear banding in steady state as previously demonstrated (Ravindranath and Wang 2008a, b; Boukany and Wang 2009a).

The present work further explores the nature of inhomogeneous breakup in entangled polybutadiene (PB) mixtures and elucidates how uneven yielding can be prevented by increasing the polymeric solvent's molecular weight. Specifically, we focus on two common modes of deformation, step strain and LAOS. We show that failure at sample/wall interfaces can be minimized by reducing the intrinsic slip length b of the mixture. Even elastic breakdown and shear banding can be completely annihilated by using a PB solvent of sufficiently high molecular weight (i.e., $M_w =$ 46 kg/mol) to prepare a 10 wt.% PB mixture. In contrast, 10 wt.% PB mixtures made with PBS of either $M_w = 1.5$ kg/mol or $M_w = 10$ kg/mol show considerable uneven structural breakdown.

Experimental

Sample preparation

Our experiments are based on three entangled 1,4-polybutadiene (PB) mixtures made with the same parent polymer ($M_w \sim 10^6$ g/mol) at 10 wt.% concentration in three different polybutadiene solvents. The molecular weights of the three PB solvents (PBS) were 1.5, 10, and 46 K respectively. The mixtures are labeled as 1 M(10%)-1.5 K, 1 M(10%)-10 K and 1 M(10%)-46 K respectively. The number of entanglements per chain $Z = M_w/M_e\phi^{-1.2}$ in each of the three mixtures is around 40, where M_w is the molecular weight of the parent polymer, M_e is the entanglement molecular weight of the pure PB equal to 1.6 kg/mol, and ϕ is the volume fraction of parent polymer. The molecular characteristics of the parent polymer and the PB solvents are listed in Table 1. The parent PB was first dissolved in excess of toluene to which PBS was added and intimately mixed. Silver-coated silica particles with an average diameter of 10 μm (Dantec Dynamics S-HGS) were first ultrasonicated in toluene and then added to the mixture with the final loading of the particles being 500–600 ppm. Most of the toluene was evaporated at room temperature under hood over a period of 2 weeks and the remaining was removed in vacuum condition until the residue is less than 0.5%.

Apparatus and particle-tracking velocimetry

All measurements were made at room temperature of around 25°C, using cone-plate geometry of $\theta = 5.4°$ and diameter of 25 mm. The overall chain relaxation time τ and mixture viscosity η_0 reported in Table 2 were obtained from small amplitude oscillatory shear frequency sweep measurements done at room temperature on an Advanced Rheometrics Expansion System (ARES). Step strain and LAOS experiments on 1 M(10%)-46 K mixture were done on ARES. All other measurements were made on a Bohlin-CVOR rheometer. Both smooth and rough surfaces were used to determine how surface condition may alter the shear responses. Rough surfaces are made by gluing sandpaper onto the cone and plate, where a small hole is left on the sandpaper surface of the stationary bottom plate for a laser sheet (cross-section of 0.2 mm × 2 mm) to pass vertically across the gap. The gap distance is determined by zeroing the gap with the sandpaper covered plates. The sandpaper is from Virginia abrasives, USA with catalog number 4687A13 and roughness of 240 grit.

The PTV consists of a CCD camera (with a maximum speed of 30 fps) placed horizontally to observe particle movements from the meniscus that is wrapped around with a transparent film. The location of the PTV measurements is at a distance of 3 to 4 mm from the meniscus of the cone-plate with 25 mm diameter. This scheme A of placing the CCD horizontally is more convenient than the scheme B involving placing the CCD at an angle and peeking through a transparent window on the stationary plate (Tapadia et al. 2006). We have shown previously that the film around the meniscus does not affect the PTV observations as long as it is made sufficiently away from the film (Tapadia et al.

Table 1 Molecular characteristics of parent PB and various PB solvents at room temperature

Sample	M_n (g/mol)	M_w (g/mol)	M_w/M_n	Source	η_s (Pa s)
1 M	1.014×10^6	1.052×10^6	1.03	University of Akron	–
PBS-1.5 K	1500	–	–	Sigma-Aldrich *Cat. No. 20,0484*	0.7
PBS-10 K	8900	10500	1.18	Bridgestone	14
PBS-46 K	45000	46000	1.02	Goodyear	2600

Table 2 Properties of PB mixtures at room temperature

Mixture	$\phi^{1.2}$ M_w/M_e	τ(s)	η_0 (Pa.s)	η_0/η_s	l_{ent} (nm)	b (mm)
1 M(10%)-1.5 K	40	17	50,000	71,428	17	1.2
1 M(10%)-10 K	40	50	1.7×10^5	12,142	17	0.2
1 M(10%)-46 K	40	75	3.9×10^5	150	17	0.002

2006). For the present step strain and LAOS, it is actually feasible to adopt the scheme B: Given the limited strain in such tests, the meniscus would remain stable. For smooth surfaces, a laser sheet was passed at an angle of ca. 45° through a glass window of 5 mm radius on the stationary plate, as depicted previously by Ravindranath and Wang (2007a, b). Movements of the illuminated particles across the entire sample thickness were captured with a black–white CCD camera placed at ca. 45°, but perpendicular to the direction of the laser. To eliminate optical reflection from the rotating steel cone, its surface was blackened using tool black mixture from Precision Brand (www.precisionbrand.com, UPC No. 45125). The CCD camera is mounted with a DIN objective lens (3.2×) through an adaptive tube (Edmund Optics: U54-868). During image analysis, the distance traveled by a particle is determined by playing 1 to 3 frames using MGI Videowave 4 software.

Interfacial failure in polymer mixtures

Table 2 reports the crucial characterization of the sample's intrinsic ability to undergo interfacial slip in terms of the slip length b. The magnitude of b is controlled by the ratio of the bulk viscosity η and viscosity η_i at the failure plane where chain entanglement is lost: $b = (\eta/\eta_i)l_{ent}$, where l_{ent} is the entanglement spacing comparable to the thickness of a disentanglement layer. Thus, the value of b can be reduced by increasing η_i whose lower bound is the solvent viscosity for entangled mixtures. Consequently, we have prepared three mixtures of equal level of chain entanglement with vastly different ability to undergo slip as shown in terms of b in Table 2. Further detailed discussion about slip extrapolation length for polymer mixtures can be found in Ravindranath and Wang (2007b).

Results and discussion

Step strain experiments

Rheological and PTV observations of step strain deformation of the three mixtures have been reported in this section. Figure 1a shows the shear stress vs. time data of five repeats on the 1 M(10%)-1.5 K mixture. The applied shear strain is $\gamma = 450\%$, produced at a Weissenberg number of $W_i = 400$. For comparison with linear response behavior, step strain data at $\gamma = 35\%$ have also been plotted in Fig. 1a. The filled symbols represent the shear stress build up during the step strain, and the open symbols are the shear stress relaxation data after shear cessation. The five repeats come from 4 different loadings, labeled as L1, L2, L3, and L4, respectively. For the fourth loading, the same step strain was repeated and labeled as L4-rep. In case of L1, L3, and L4-rep, the mixture was allowed to relax for nearly 12 h before the step strain experiments were performed and in case of L2 and L4, the mixture was relaxed for 3 h after loading.

The stress relaxation characteristics show excellent overlapping among the five data sets. Such phenomenology made sure that no discrepancy can be rheologically apparent. In situ PTV observations show in Fig. 1b that the step-strained samples did not relax quiescently. In the case of L1, L2, L4, and L4-rep, the samples appear to suffer interfacial failure that allowed the residual stress to decline faster than quiescent chain relaxation would cause. In other words, the traced particles near the two interfaces made maximum movements, as much as 600 to 800 μm, after shear cessation.

It is statistically significant with enough repeats that the sample disintegration may be different in each sample loading. For example, a detailed PTV analysis reveals in Fig. 1c that internal failure occurs for L3. Maximum relative movements of the traced particles are observed to take place at two locations as indicated. In some of the repeats, Y-motion of a few particles was also observed on the order of 20–30 μm. More importantly, the PTV observations in Fig. 1c show that most of the movements occur within the first 10 s after shear cessation, which is consistent with the initial faster stress decline shown in Fig. 1a. On the other hand, no discernible motions can be seen for the small step strain of $\gamma = 35\%$.

The 1 M(10%)-1.5 K mixture tends to undergo interfacial failure because it has a sizable slip length b. With b comparable to the sample thickness, interfacial slip can cause quick macroscopic recoil, resulting in accelerated stress relaxation (Ravindranath and Wang 2007a,

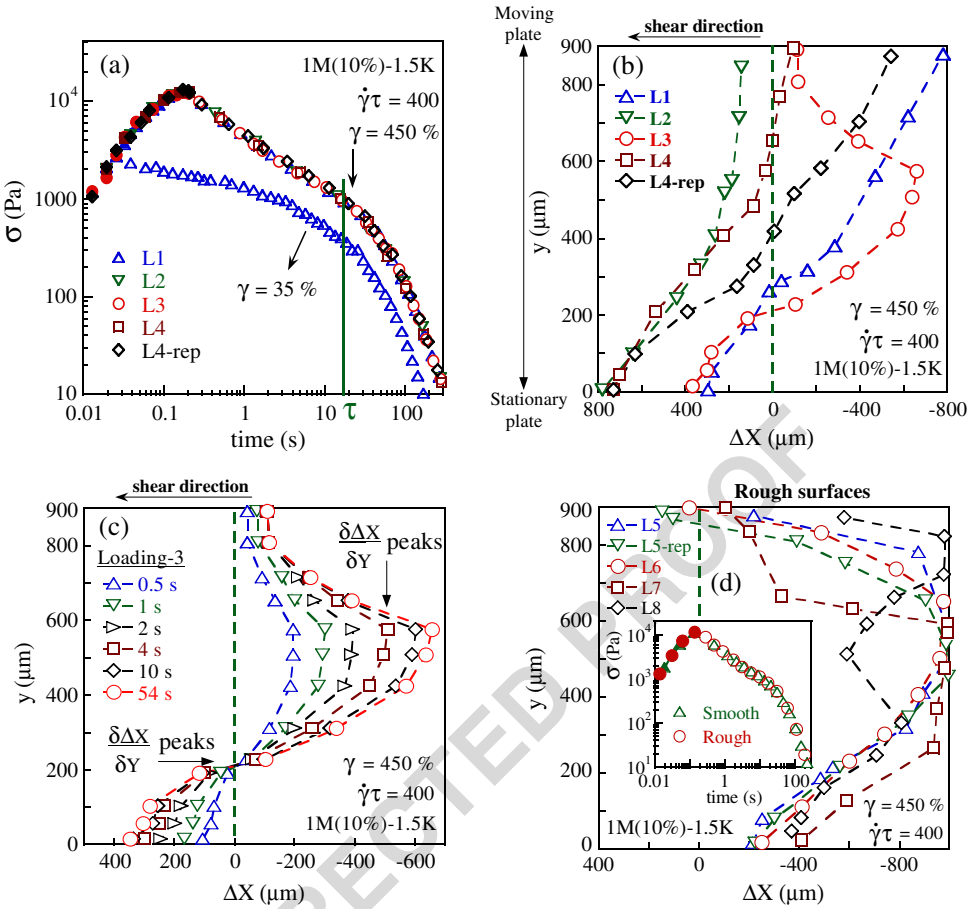

Fig. 1 **a** Shear stress vs. time plot of 5 step strain experimental repeats of 1 M(10%)-1.5 K mixture. L1, L2, L3, and L4 correspond to four different loadings and L4-rep corresponds to the repeat experiment of the fourth loading. *Closed symbols* indicate build up of shear stress during deformation, while open symbols are stress relaxation data. The step strain is produced at a Weissenberg number $Wi = 400$. Both the surfaces were smooth unlike in Fig. 1e and Fig. 4d, where the surfaces were rough. **b** Total displacement of tracer particles across the gap after cessation of step deformation for 5 repeats as observed through PTV. **c** Displacement of tracer particles across the gap at different times after cessation of step deformation for loading-3 (L3) as observed through PTV. The two surfaces are smooth. **d** Total displacement of tracer particles across the gap after cessation of step deformation for five repeats of four different loadings. Both the surfaces were roughened by gluing sandpaper. PTV was done by placing the camera horizontally and viewing through the edge. *Inset* shows the rheological response of the mixture with smooth and rough surfaces

b). Majority of the previous cases in the literature, employed either small molecular organic liquids or low molecular weight oligomers to make well-entangled PS or PB mixtures (Einaga et al. 1971; Fukuda et al. 1975; Osaki and Kurata 1980; Vrentas and Graessley 1982; Larson et al. 1988; Archer et al. 1995, 2002; Sanchez-Reyes and Archer 2002; Islam et al. 2001, 2003; Venerus and Nair 2006; Wen and Hua 2009). In all of these cases, owing to large values of interfacial slip length b, significant interfacial failure may take place after shear cessation similar to the one shown in Fig. 1b.

Sanchez-Reyes and Archer (2003) have shown that surface roughness could minimize wall slip. Thus, it seems a reasonable idea to examine the effect of surface roughness on the phenomenon of non-quiescent relaxation after step strain for the present sample.

Figure 1d shows the PTV measurements of the same step strain as depicted in Fig. 1a–c except that the surfaces of the cone and plate are made of sandpapers. It can be clearly seen from Fig. 1d that for the five repeats from four separate loadings, largest displacement and maximum relative movements both occur in the sample interior. Thus, the sandpaper has largely removed the chance for the step-strained sample to undergo (entanglement) network disintegration at the interface between the sample and the shear surface, leaving the sample no choice but to suffer structural breakdown in the sample interior. It is important to

observe that despite the apparent difference in the failure locations the stress relaxation signals are the same for both smooth and rough surfaces as shown in the inset.

The elastic yielding behavior observed in Fig. 1a–d is expected to depend on the "slip characteristics". Table 2 shows that 1 M(10%)-10 K has much reduced ability to undergo wall slip. So let us contrast its behavior under the same step strain with the previous sample. Figure 2a and b show respectively the rheological behavior and corresponding in situ PTV observations in five repeats. Again, the rheological responses of all five repeats are identical, involving accelerated stress decline relative to that from a step strain of $\gamma = 100\%$. Although the rheological character is indistinguishable from that of the 1 M(10%)-1.5 K, the PTV observations in Fig. 2b indicate that interfacial failure is largely removed by employing the PBS of higher molecular weight.

Further increasing the molecular weight of the polybutadiene solvent (PBS) to 46 kg/mol, which is a well-entangled melt itself, we give the 1 M(10%)-46 K mixture with little ability to make any sizable interfacial or internal slip. Consider a large step strain (i.e., $\gamma = 450\%$): Upon shear cessation, the residual elastic retraction force overcomes the entanglement (cohesion) force to cause disentanglement (Wang et al. 2007a, b) over a length scale given by the entanglement spacing $l_{ent} \sim \phi^{-1.2} M_e$. Let us estimate the amount of displacement due to this disentanglement and determine whether it would result in significant macroscopic (elastic) recoil. Assume that the mutual chain sliding in the entanglement-free layer of thickness l_{ent} corresponds to a "slip velocity" V_s at shear stress σ. This disentanglement layer of viscosity η_i would be sheared at a rate of V_s/l_{ent} so that $\eta_i(V_s/l_{ent}) = \sigma$. Let us assume that this displacement would last for a period of Δt, leading to $\Delta x \sim V_s \Delta t = (l_{ent}\sigma/\eta_i)\Delta t$. Here, the level of shear stress σ can be evaluated approximately according to $\sigma \sim G\gamma = (\eta/\tau)\gamma$ for a sudden step strain of γ. Thus, we have $\Delta x \sim b\,\gamma(\Delta t/\tau)$, where $b = (\eta/\eta_i)l_{ent}$, and τ is the terminal relaxation time. It is clear that Δt cannot exceed τ, beyond which the diffusion-dominated relaxation would occur. Thus, the displacement would only last for $\Delta t < \tau$. We consequently conclude for $b/H << 1$ that the recoil measured in terms of a strain $\Delta\gamma_s \sim \Delta x/H$ is negligibly small, relative to the imposed strain because $\Delta\gamma_s/\gamma < (b/H) << 1$. The third mixture of 1 M(10%)-46 K is designed to have $b \sim 2\ \mu m << H \sim 1$ mm. Therefore, any disentanglement starting on a length scale of l_{ent} would not produce significant motions and would not appreciably accelerate stress relaxation. As consequence, the rest of the sample would retain the same amount of residue shear stress. In other words, no part of the sample would be singled out to undergo cohesive breakdown, and disentanglement could only evolve democratically and uniformly throughout the sample.

Because of the PBS' high molecular weight of 46 kg/mol and corresponding solvent viscosity, Fig. 3a shows an initial stress drop due to the viscous stress associated with the PBS of, which is a smaller fraction of the total residual stress for $\gamma = 350\%$ than for $\gamma = 35\%$. The stress relaxation following $\gamma = 350\%$ is

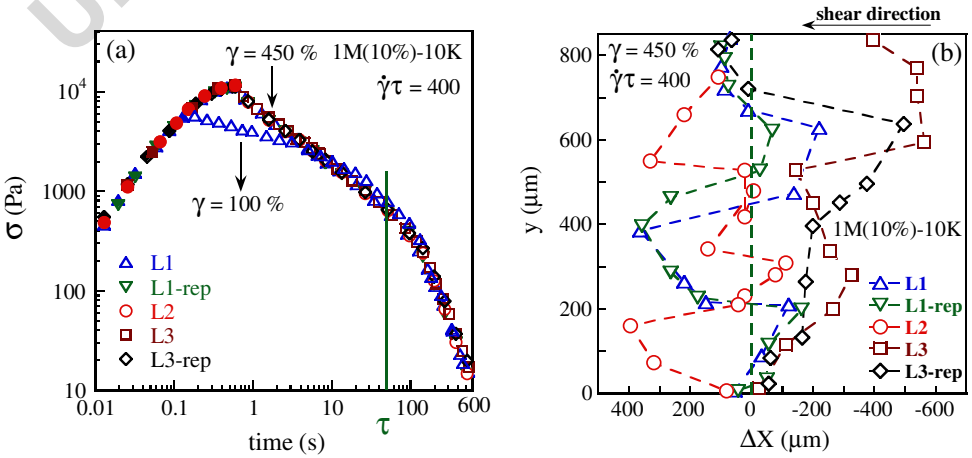

Fig. 2 **a** Shear stress vs. time plot of five-step strain experimental repeats of 1 M(10%)-10 K mixture. L1, L2, and L3 correspond to three different loadings. L1-rep and L3-rep corresponds to the repeat experiment of the first and third loading. *Closed symbols* indicate build up of shear stress during deformation, while *open symbols* are stress relaxation data. Both the surfaces are smooth. **b** Total displacement of tracer particles across the gap after cessation of step deformation for five repeats of three loadings as observed through PTV

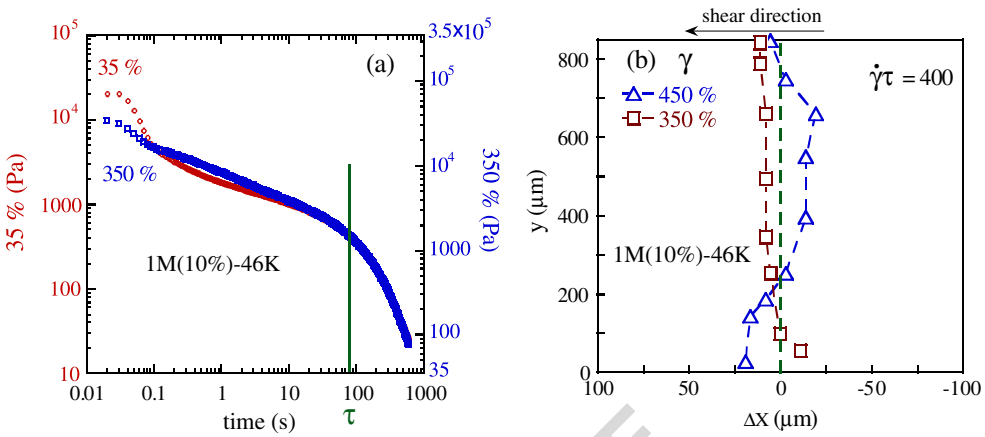

Fig. 3 **a** Relaxing shear stress vs. time for strains of 35% and 350%. **b** Total displacement of tracer particles across the gap after cessation of step deformation as observed through PTV. Both the surfaces are smooth

compared with the linear relaxation behavior for $\gamma =$ 35% by matching the stress level around the dominant relaxation dynamics at τ, using double Y axes. The mismatch on the time scales ranging from 0.1 to 10 s is real and arises from the fact that the small step strain of 35% allows less stress relaxation during shear and consequently contains a fuller spectrum of relaxation dynamics, particularly some faster relaxing components in the shear stress. Figure 3b indicates that macroscopic motion is greatly reduced after step strain at both $\gamma =$ 350% and 450%. In absence of significant macroscopic motions after shear cessation, the stress decrease with time is not much different from what is observed in the linear response regime. Actually, as noted above, the stress decline is less rapid over the period from 0.1 to 10 s.

Large amplitude oscillatory shear

LAOS has been also been used as a tool to probe the nonlinear behavior of entangled polymer mixtures and melts (Adrian and Giacomin 1992; Reimers and Dealy 1996; Wilhelm 2002; Debbaut and Burhin 2002; Clemeur et al. 2003; Schlatter et al. 2005). Various analyses have been applied to extract useful information from LAOS measurements, including Fourier analysis (Wilhelm et al. 1999, 2000; Dusschoten et al. 2001; Kallus et al. 2001; Karis et al. 2002; Neidhofer et al. 2003, 2004; Sim et al. 2003) geometric aspect of viscoelasticity (Cho et al. 2005), network model (Giacomin and Oakley 1992; Yosick et al. 1997; Sim et al. 2003; Jeyaseelan and Giacomin 2008), Berstein, Kearsley, and Zapas (BKZ) model (Giacomin et al. 1993) and molecular stress function model (Wapperom et al. 2005). When analyzing the origin of the nonlinearities such as the stress wave distortions, many of such studies (e.g., Giacomin and Oakley 1992; Reimers and Dealy 1996; Jeyaseelan and Giacomin 2008; Yu et al. 2009) assume that homogeneous deformation prevails during LAOS. To properly explain how the wave distortion occurs using any model, we first need to know from experiment whether LAOS involves homogeneous deformation or not (Li et al. 2009), and secondly we have to use a model that permits shear inhomogeneity. The analyses themselves, such as the FT analysis by Wilhelm et al. (1999) and analytical treatments by Cho et al. (2005), Ewoldt et al. (2009) and Yu et al. (2009), cannot reveal whether shear inhomogeneity occurred or not (Rouyer et al. 2008). To determine from the rheometric data whether shear banding occurs in LAOS, one first would have to have a constitutive model that can faithfully depict shear inhomogeneity in LAOS. Even then, in our opinion, there is no one-to-one correspondence to allow one to characterize any strain localization based only on the rheometric information although Klein et al. (2007) tried to do so. For these reasons, we focus on the experimental determination of whether the LAOS is homogeneous or not.

In this section, we report rheological and PTV observations of the three entangled polymer mixtures under LAOS. Velocity profiles at the instant of 5/8th cycle of an oscillatory wave in steady state (when shear stress response is steady) are presented in Fig. 4a for the 1 M(10%)-1.5 K mixture in five repeats. The five repeats come from four different loadings L9, L10, L11, and L12. L9-rep refers to a repeated experiment of the ninth loading-L9. Each of the experiments was done 3 h after the sample loading. The applied strain γ_0 is 175% and frequency ω is 3 rad/s, corresponding to a Deborah number of $\omega\tau \sim 51$. At the instant of 5/8th cycle, the average shear rate across the gap is 3.7 s^{-1}. It can be noted from Fig. 4a that interfacial failure is observed in case of L9 and L11, while bulk banding can also be seen along with the interfacial failure in case of L9-rep, L10 and L12. Similar to the preceding PTV observations of step strain, the repeats present quite different velocity

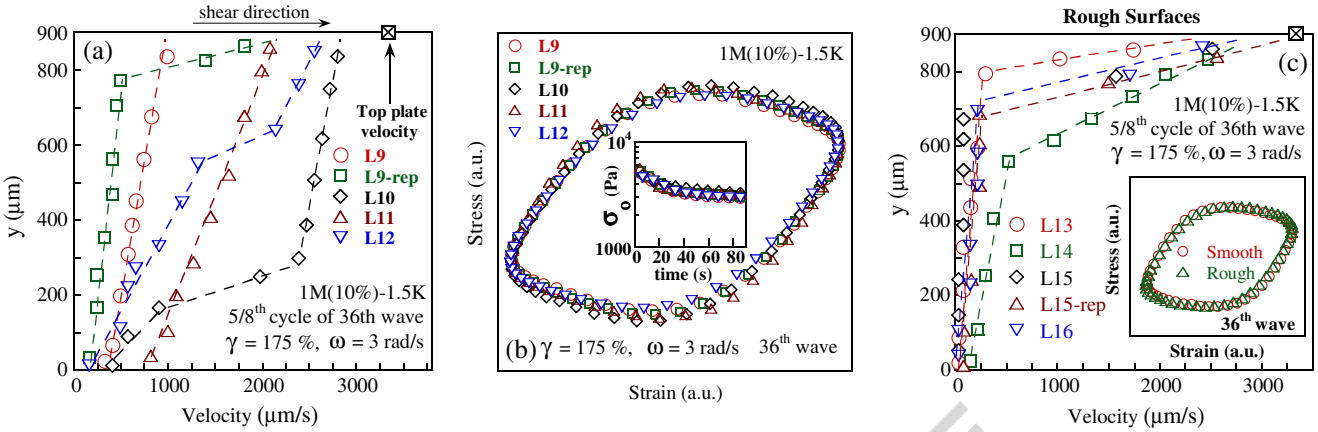

Fig. 4 **a** Velocity profiles at the instant of 5/8th cycle of 36th wave (74.6 s) of five repeat experiments based on four different loadings on smooth surfaces of cone and plate. The applied strain γ is 175% and oscillation frequency ω is 3 rad/s. The *crossed square symbol* indicates the velocity of the top moving plate. **b** Lissajous plot of 36th wave of the five repeat experiments, where the stress voltage signal is plotted against strain voltage signal. The *inset* shows the maximum stress vs. time data of the five repeat experiments as directly given by the rheometer. **c** Velocity profiles at the instant of 5/8th cycle of 36th wave (74.6 s) of five repeat experiments of four different loading L13, L14, L15, and L16. By gluing sandpaper, both the surfaces were roughened. PTV was done by placing the camera horizontally and viewing through the edge. The *inset* shows the Lissajous plot of 36th wave with the smooth and rough surfaces

profiles. Yet, the rheological measurements essentially overlap as shown in Fig. 4b. In Fig. 4b, the Lissajous plot of 36th wave of the five repeats has been presented along with the inset showing peak shear stress vs. time data read from the rheometer. The strong distortion observed in the Lissajous plot indicates that the system is alternating between different states of viscoelasticity within each cycle. This alternation does not have to involve shear banding. But when it does, it explicitly reveals why the stress wave distorted. Moreover, in presence of shear inhomogeneity, we need to bear in mind the strain used in making the Lissajous plots is only the nominal or the apparent strain. This note is worthwhile whenever one starts to think about such plots in terms of any particular constitutive model.

Figure 4c presents the PTV observations made with two rough (sandpaper covered) surfaces. Apparently, on rough surfaces, significant bulk shear banding can take place during LAOS even for this mixture that is inherently capable of significant wall slip. Since our PTV does not have sufficient resolution to distinguish shear banding of immeasurably small thickness at the interface from true wall slip, the appreciable shear band width produced with the rough surfaces is insightful and significant.

The PTV observations of 1 M(10%)-10 K entangled mixture under LAOS is shown in Fig. 5. The applied strain γ_0 is 175% and the oscillation frequency is 1 rad/s. For all five repeats based on three separate loadings, strong shear banding can be observed in the bulk. In the case of loading-6 (L6), some failure at the bottom interface can be seen along with bulk banding. Use of 10 K PB as the solvent produces a marked difference in the deformation field profiles during LAOS by comparison between Figs. 4a and 5. The tendency to fail at the interfaces as in the case of 1.5 K mixture is effectively removed in 1 M(10%)-10 K.

Finally, it is instructive to examine the consequence of further increasing the molecular weight of PBS.

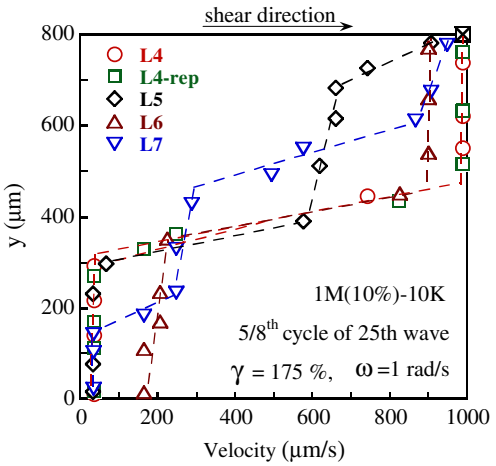

Fig. 5 Velocity profiles at the instant of 5/8th cycle of 25th wave (154.6 s) of 5 repeat experiments of 4 different loading L4, L5, L6, and L7. The applied strain γ is 175% and frequency ω is 1 rad/s. The two surfaces are smooth

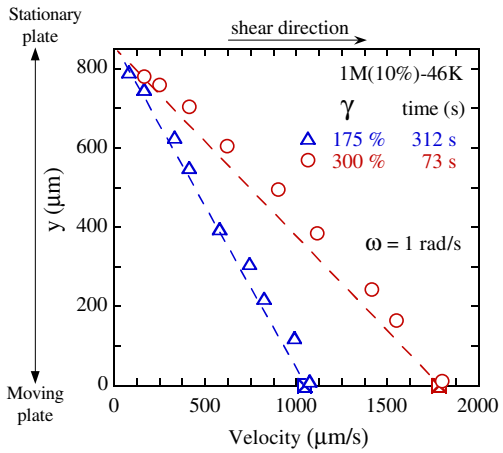

Fig. 6 Velocity profiles at the instant of 5/8th cycle based on smooth surfaces. The applied strain γ_0 is 175% and 300% at frequency ω of 1 rad/s. The velocity profile is basically linear at all other moments of the cycle

In the preceding subsection we already demonstrated how PBS of $M_w = 46$ kg/mol suppressed large macroscopic motions after step strain. Figure 6 reveals, at all time, homogeneous LAOS essentially prevails in the 1 M(10%)-46 K mixture for two values of the amplitude. This sample is able to evolve toward its steady state without developing any inhomogeneous structural change. The stress level hardly changed for $\gamma_0 = 175\%$ over time, and dropped no more than 10% for $\gamma = 300\%$.

Summary

The important role of the PBS in controlling the nonlinear rheological responses of PB mixtures to step strain and LAOS has been elucidated. Equally important is the demonstration of the effectiveness of rough surfaces in altering the location of structural failure in the 1 M(10%)-1.5 K mixture that has strong inclination to undergo wall slip (i.e., interfacial failure). At the same level of chain entanglement, the three mixtures made with PBS of different molecular weights show significant different responses to external deformation. Different repeats even produced different deformation profiles. Yet, the rheological characteristics, i.e., the stress responses, remain the same in both step strain and LAOS.

In short, there are five important findings of the present work. (a) Different states of material deformation correspond to the same rheological characteristics. (b) Large deformation produces structural inhomogeneity whose spatial characteristics may not be predictable. (c) Surface roughness can effectively eliminate slip-like interfacial failure allowing bulk shear banding to prevail. (d) The high molecular weight polymeric solvent (PBS) saves the entangled PB solution from undergoing severe interfacial failure. (e) The PBS of highest molecular weight (46 kg/mol) actually can suppress inhomogeneous yielding in both step strain and during LAOS. These observations greatly improve our current understanding of nonlinear rheological responses of well-entangled polymeric liquids and are the first step toward depicting how polydispersity in the molecular weight distribution might influence the state of deformation and flow.

Acknowledgement This research is supported, in part, by a grant (DMR-0821697) from the National Science Foundation.

References

Adrian DW, Giacomin AJ (1992) The quasi-periodic nature of a polyurethane melt in oscillatory shear. J Rheol 36:1227–1243

Archer LA, Chen YL, Larson RG (1995) Delayed slip after step strains in highly entangled polystyrene mixtures. J Rheol 39:519–525

Archer LA, Sanchez-Reyes J, Juliani (2002) Relaxation dynamics of polymer liquids in nonlinear step strain. Macromolecules 35:10216–10224

Boukany PE, Wang SQ (2007) A correlation between velocity profile and molecular weight distribution in sheared entangled polymer mixtures. J Rheol 51:217–233

Boukany PE, Wang SQ (2009a) Shear banding or not in entangled DNA mixtures depending on the level of entanglement. J Rheol 53:73–83

Boukany PE, Wang SQ, Wang XR (2009b) Step strain of entangled linear polymer melts: new experimental evidence for elastic yielding. Macromolecules 42:6261–6269

Boukany PE, Wang SQ (2009c) Exploring origins of interfacial yielding and wall slip in entangled linear melts during shear or after shear cessation. Macromolecules 42:2222–2228

Cho KS, Hyun K, Ahn KH, Lee SJ (2005) A geometrical interpretation of large amplitude oscillatory shear response. J Rheol 49:747–758

Clemeur N, Rutgers RPG, Debbaut B (2003) On the evaluation of some differential formulations for the pom-pom constitutive model. Rheol Acta 42:217–231

Debbaut B, Burhin H (2002) Large amplitude oscillatory shear and Fourier-transform rheology for a high density polyethylene: experiments and numerical simulation. J Rheol 46:1155–1176

Dusschoten DV, Wilhelm M, Spiess HW (2001) Two-dimensional Fourier transform rheology. J Rheol 45:1319–1339

Einaga Y, Osaki K, Kurata M, Kimura S, Tamura M (1971) Stress relaxation of polymer mixtures under large strain. J Polym 2:550–552

Ewoldt RH, Hosoi AW, McKinley GH (2009) New measures for characterizing nonlinear viscoelasticity in large amplitude oscillatory shear. J Rheol 52:1427–1458

Fukuda M, Osaki K, Kurata M (1975) Nonlinear viscoelasticity of polystyrene mixtures. I. Strain-dependent relaxation modulus. J Polym Sci, Polym Phys Ed 13:1563–1576

Giacomin AJ, Oakley JG (1992) Structural network models for molten plastics evaluated in large-amplitude oscillatory shear. J Rheol 36:1529–1546

Giacomin AJ, Jeyaseelan RS, Samurkas T, Dealy JM (1993) Validity of separable BKZ model for large amplitude oscillatory shear. J Rheol 37:811–826

Graessley WW (2008) Polymeric liquids and networks: dynamics and rheology. Garland, London

Hu YT, Wilen L, Philips A, Lips A (2007) Is the constitutive relation for entangled polymers monotonic? J Rheol 51:275–295

Islam MT, Sanchez-Reyes J, Archer LA (2001) Nonlinear rheology of highly entangled polymer liquids: step strain damping function. J Rheol 45:61–82

Islam MT, Sanchez-Reyes J, Archer LA (2003) Step and steady shear responses of nearly monodisperse highly entangled 1,4-polybutadiene mixtures. Rheol Acta 42:191–198

Jeyaseelan RS, Giacomin AJ (2008) Network theory for polymer solutions in large amplitude oscillatory shear. J Non-Newton Fluid Mech 148:24–32

Juliani, Archer LA (2001) Linear and nonlinear rheology of bidisperse polymer blends. J Rheol 45:691–708

Kallus S, Willenbacher N, Kirsch S, Distler D, Neidhofer T, Wilhelm M, Spiess HW (2001) Characterization of polymer dispersions by Fourier transform rheology. Rheol Acta 40:552–559

Karis TE, Seymour CM, Kono RN, Jhon MS (2002) Harmonic analysis in rheological property measurement. Rheol Acta 41:471–474

Keesha AH, Buckley MR, Cohen I, Archer LA (2008) High remixture shear profile measurements in entangled polymers. Phys Rev Lett 101:218301

Keesha AH, Buckley MR, Qi H, Cohen I, Archer LA (2010) Constitutive curve and velocity profile in entangled polymers during start-up of steady shear flow. Macromolecules 43:4412–4417

Klein CO, Spiess HW, Calin A, Balan C, Wilhelm M (2007) Separation of the nonlinear oscillatory response into a superposition of linear, strain hardening, strain softening, and wall slip response. Macromolecules 40:4250–4259

Larson RG, Khan SA, Raju VR (1988) Relaxation of stress and birefringence in polymers of high molecular weight. J Rheol 32:145–161

Li X, Wang SQ, Wang XR (2009) Nonlinearity in large amplitude oscillatory shear (LAOS) of different viscoelastic materials. J Rheol 53:1255–1274

Macosko CW (1994) Rheology: principles, measurements and applications. Wiley, New York.

Neidhofer T, Wilhelm M, Debbuat B (2003) Fourier-transform rheology experiments and finite-element simulations on linear polystyrene mixtures. J Rheol 47:1351–1371

Neidhofer T, Sioula S, Hadjichristidis N, Wilhelm M (2004) Distinguishing linear from star-branched polystyrene mixtures with Fourier-transform rheology. Macromol Rapid Commun 25:1921–1926

Osaki K, Kurata M (1980) Experimental appraisal of the Doi–Edwards theory for polymer rheology based on the data for polystyrene mixtures. Macromolecules 13:671–676

Ravindranath S, Wang SQ (2007a) Steady state measurements in stress plateau region of entangled polymer mixtures: controlled-rate and controlled-stress modes. J Rheol 40:8031–8039

Ravindranath S, Wang SQ (2007b) What are the origins of stress relaxation behaviors in step strain of entangled polymer mixtures? Macromolecules 40:8031–8039

Ravindranath S, Wang SQ (2008a) Large amplitude oscillatory shear behavior of entangled polymer mixtures: particle tracking velocimetric investigation. J Rheol 52:341–358

Ravindranath S, Wang SQ, Olechnowicz M, Quirk RP (2008) Banding in simple steady shear of entangled polymer mixtures. Macromolecules 41:2663–2670

Reimers MJ, Dealy JM (1996) Sliding plate rheometer studies of concentrated polystyrene mixtures: large amplitude oscillatory shear of a very high molecular weight polymer in diethyl Phthalate. J Rheol 40:167–186

Rouyer F, Cohen-Addad S, Höhler R, Sollich P, Fielding SM (2008) The large amplitude oscillatory strain response of aqueous foam: strain localization and full stress Fourier spectrum. Eur Phys J E 27:309–321

Sanchez-Reyes J, Archer LA (2002) Step strain dynamics of entangled polymer liquids. Macromolecules 35:5194–5202

Sanchez-Reyes J, Archer LA (2003) Interfacial slip violations in polymer mixtures: role of microscale surface roughness. Langmuir 19:3304–3312

Schlatter G, Fleury G, Muller R (2005) Fourier transform rheology of branched polyethylene: experiments and models for assessing the macromolecular architecture. Macromolecules 38:6492–6503

Sim HG, Ahn KH, Lee SJ (2003) Large amplitude oscillatory shear behavior of complex fluids investigated by a network model: a guideline for classification. J Non-Newton Fluid Mech 112:237–250

Tapadia P, Wang SQ (2006) Direct visualization of continuous simple shear in non-Newtonian polymeric fluids. Phys Rev Lett 96:016001

Tapadia P, Ravindranath S, Wang SQ (2006) Banding in entangled polymer fluids under oscillatory shearing. Phys Rev Lett 96:196001

Venerus DC, Nair R (2006) Stress relaxation dynamics of an entangled polystyrene mixture following step strain flow. J Rheol 50:59–75

Vrentas CM, Graessley WW (1982) Study of shear stress relaxation in well characterized polymer liquids. J Rheol 26:359–371

Wang SQ, Ravindranath S, Boukany P, Olechnowicz M, Quirk R, Halasa A, Mays J (2006) Non-quiescent relaxation of entangled polymeric liquids after step strain. Phys Rev Lett 97:187801

Wang Y, Wang SQ, Boukany PE, Wang X (2007a) Elastic breakup in uniaxial extension of entangled polymer melts. Phys Rev Lett 99:237801

Wang SQ, Ravindranath S, Wang Y, Boukany PE (2007b) New theoretical considerations in polymer rheology: elastic breakdown of chain entanglement network. J Chem Phys 127:064903

Wapperom P, Leygue A, Keunings R (2005) Numerical simulation of large amplitude oscillatory shear of a high-density polyethylene melt using the MSF model. J Non-Newton Fluid Mech 130:63–76

Wen YH, Hua CC (2009) Chain stretch and relaxation in transient entangled mixtures probed by double-step strain flow. J Rheol 53:781–798

Wilhelm M (2002) Fourier-transform rheology. Macromol Mater Eng 287:83–105

Wilhelm M, Reinheimer P, Ortseifer M (1999) High sensitivity Fourier-transform rheology. Rheol Acta 38:349–356

Wilhelm M, Reinheimer P, Ortseifer M, Neidhofer T, Spiess HW (2000) The crossover between linear and non-linear mechanical behavior in polymer mixtures as detected by Fourier-rheology. Rheol Acta 39:241–246

Yosick JA, Giacomin AJ, Moldenaers P (1997) A kinetic network model for nonlinear flow behavior of molten plastics in both shear and extension. J Non-Newton Fluid Mech 70:103–123

Yu W, Wang P, Zhou CX (2009) General stress decomposition in nonlinear oscillatory shear flow. J Rheol 53:215–238